

# Application of magnetic resonance computer-aided diagnosis for preoperatively determining invasive disease in ultrasonography-guided core needle biopsy-proven ductal carcinoma in situ

Hye Shin Ahn, MD<sup>a</sup>, Sun Mi Kim, MD<sup>b,\*</sup> , Mi Sun Kim, MD<sup>c</sup>, Mijung Jang, MD<sup>b</sup>, Bo La Yun, MD<sup>b</sup>, Eunyong Kang, MD<sup>d</sup>, Eun-Kyu Kim, MD<sup>d</sup>, So Yeon Park, MD<sup>e</sup>, Bohyoung Kim, PhD<sup>f</sup>

## Abstract

The aim of this study was to analyze kinetic and morphologic features using dynamic contrast-enhanced magnetic resonance imaging (DCE-MRI) with computer-aided diagnosis (CAD) to predict occult invasive components in cases of biopsy-proven ductal carcinoma in situ (DCIS).

We enrolled 138 patients with 141 breasts who underwent preoperative breast MRI and were diagnosed with DCIS via ultrasonography (US)-guided core needle biopsy performed at our institution during January 2009 to December 2012. Their clinical, mammographic, ultrasonographic, MRI, and final histologic findings were retrospectively reviewed. Their mammographic, ultrasonographic, and MRI findings were analyzed according to the American College of Radiology Breast Imaging Reporting and Data System. CAD findings of detectability, initial (fast, medium, and slow) and delay (persistent, plateau, and washout) phase enhancement kinetic descriptor, peak enhancement percentage, and lesion size were evaluated. Continuous and categorical variables were analyzed using independent *t* test and  $\chi^2$  or Fisher exact test, respectively. Independent factors for predicting the presence of invasive component were evaluated by multivariate logistic regression analysis.

Final histologic findings revealed that 55 breasts (39%) had DCIS with an invasive component. MRI-detected, CAD-detected, or pathologic lesion size ( $P = .002$ ,  $P = .001$ ,  $P < .001$ , respectively), delay washout kinetics and detectability on CAD ( $P < .001$  and  $P = .004$ , respectively), presence of symptoms ( $P = .01$ ), presence of comedonecrosis ( $P < .001$ ), nuclear grade ( $P = .001$ ), abnormality on mammography ( $P = .02$ ), or US ( $P = .03$ ) were significantly different between pure DCIS and the DCIS with an invasive component group on univariate analysis. Of those findings, multivariate analysis revealed that delay washout on CAD (odds ratio [OR], 4.36; 95% confidence interval [CI], 1.96–9.69;  $P = .0003$ ) and pathologic size (OR, 1.29; 95% CI 1.05–1.57;  $P = .014$ ) were independent predictive factors for the presence of an invasive component.

Delay washout kinetic features measured by CAD and pathologic tumor size are potentially useful for predicting occult invasion in cases of biopsy-proven DCIS.

Breast MRI including a CAD system would be helpful for predicting invasive components in cases of biopsy-proven DCIS and for selecting patients for sentinel lymph node biopsy.

**Abbreviations:** CAD = computer-aided diagnosis, DCIS = Ductal carcinoma in situ, MRI = magnetic resonance imaging, US = ultrasonography.

**Keywords:** breast lesion, breast MRI, CAD, ductal carcinoma in situ

Editor: Maya Saranathan.

This research was supported by Basic Science Research Program through the National Research Foundation of Korea(NRF) funded by the Ministry of Education(No. 2017R1D1A1B03033975).

The authors report no conflicts of interest.

The datasets generated during and/or analyzed during the current study are available from the corresponding author on reasonable request.

<sup>a</sup> Department of Radiology, Chung-Ang University Hospital, Chung-Ang University College of Medicine, Seoul, <sup>b</sup> Department of Radiology, Seoul National University Bundang Hospital, Seoul National University College of Medicine, Seongnam, Gyeonggi, <sup>c</sup> Department of Radiology, Joint Heal Hospital, Seoul, <sup>d</sup> Department of Surgery, <sup>e</sup> Department of Pathology, Seoul National University Bundang Hospital, Seoul National University College of Medicine, Seongnam, Gyeonggi, <sup>f</sup> Division of Biomedical Engineering, Hankuk University of Foreign Studies, Gyeonggi-do, Republic of Korea.

\* Correspondence: Sun Mi Kim, Department of Radiology, Seoul National University Bundang Hospital, Seoul National University College of Medicine, Gumi-dong, Bundang-gu, Seongnam-si, Gyeonggi-do 463-707, Korea (e-mail: kimsmlms@daum.net).

Copyright © 2020 the Author(s). Published by Wolters Kluwer Health, Inc.

This is an open access article distributed under the terms of the Creative Commons Attribution-Non Commercial License 4.0 (CCBY-NC), where it is permissible to download, share, remix, transform, and buildup the work provided it is properly cited. The work cannot be used commercially without permission from the journal.

How to cite this article: Ahn HS, Kim SM, Kim MS, Jang M, La Yun B, Kang E, Kim EK, Park SY, Kim B. Application of magnetic resonance computer-aided diagnosis for preoperatively determining invasive disease in ultrasonography-guided core needle biopsy-proven ductal carcinoma in situ. *Medicine* 2020;99:31(e21257).

Received: 14 February 2020 / Received in final form: 1 May 2020 / Accepted: 12 June 2020

<http://dx.doi.org/10.1097/MD.00000000000021257>

## 1. Introduction

Since the increased implementation of screening programs, approximately 20% to 25% of the screening-detected breast cancers have been ductal carcinoma in situ (DCIS).<sup>[1,2]</sup> DCIS reportedly changes to become an invasive cancer at a likelihood of 30% to 50%.<sup>[3]</sup> Core-needle biopsy is usually performed to diagnose DCIS, but the underestimation rate is up to 59% compared with the final excisional pathologic examination.<sup>[4,5]</sup> Preoperative prediction of invasive components for biopsy-proven DCIS is important because of the sentinel lymph node biopsy (SLNB) procedure required for invasive cancer.<sup>[6]</sup> It is controversial to perform an SLNB procedure for all biopsy-proven pure DCIS patients due to the possibility of overtreatment.<sup>[7]</sup> Currently, noninvasive imaging studies, particularly MRI-based studies, are widely being performed to evaluate cancer stage and discriminate benign from malignant lesions.

On dynamic contrast-enhanced (DCE) MR images, pure DCIS lesions often appear as nonmass clumped areas of enhancement with segmental or linear distribution.<sup>[8,9]</sup> The reported kinetic findings of pure DCIS vary, involving plateaus, washouts, or persistent enhancement curves<sup>[8,9]</sup>; however, a recent report stated that the plateau enhancement curve was the dominant kinetic pattern for pure DCIS.<sup>[10]</sup> Recent studies have attempted to find useful features of breast MRI to predict occult invasion in biopsy-proven DCIS.<sup>[11–13]</sup> However, the results varied and every author described different significant features such as high signal intensity on T2-weighted imaging of nonmass enhancement (NME), lesion size, or mass on MRI scans.<sup>[11–13]</sup>

DCE MRI may be useful in primary surgical planning but visual assessment with DCE MRI has many inter- and intra-observer variations. Computer-aided diagnosis (CAD) can reduce these variations with objective evaluation of breast lesions.<sup>[14,15]</sup> To the best of our knowledge, no study in the literature has used CAD to date for predicting occult invasion in biopsy-proven pure DCIS. Our hypothesis is that CAD findings can be used to predict occult invasive components in biopsy-proven pure DCIS.

This study aims to analyze kinetic and morphological features using DCE MRI with CAD for predicting invasive components in cases of biopsy-proven DCIS.

## 2. Material and methods

Institutional review board approval was obtained at Seoul National University Bundang Hospital (SNUBH) (IRB-B-2001-588-101) and informed consent was not required because of the study's retrospective nature.

### 2.1. Lesion and patient characteristics

From January 2009 to December 2012, 222 breasts of 209 patients diagnosed with DCIS via ultrasonography (US)-guided core needle biopsy at our institution were enrolled. Of those, 141 breast cancers of 138 patients (three patients had bilateral cancers) were finally included with the following inclusion criteria: patients who underwent a breast MRI before surgery; patients with an available CAD result associated with breast MRI; patients with a surgically confirmed pathology; and patients who did not undergo preoperative chemotherapy.

All patients were women and their ages were in the range of 25 to 76 years, with an average age of 51.1 years. Their clinical symptoms were variable including palpable mass (n=33),

discharge (n=8), and pain (n=3). Asymptomatic screening MMG (n=75) or US (n=19) abnormalities were also present. All women underwent 2-view mammography (craniocaudal and mediolateral oblique views) using a full-field digital mammography system (Senographe 2000D FFDM; GE Medical Systems, Buc, France) and breast US (HDI 5000 or IU22, Philips-Advanced Technology Laboratories, Bothell, WA) before undergoing breast MRI, and the patients underwent MR examination after being diagnosed with DCIS based on the results of a US-guided core needle biopsy performed using a 14-gauge automated biopsy gun (STERICUT, TSK Laboratory, Tochigi, Japan). The mean number of cores for 14-G core needle biopsy was 5. In the case of calcified lesions, specimen radiography was obtained to confirm calcification retrieval. US-guided core needle biopsy of lesions was performed by one of the 3 radiologists (10–13, 3–6 years, and 1–4 years of breast imaging experience, respectively).

### 2.2. Breast MR protocol and CAD application

MRIs were performed with a 3 T Philips Achieva (Philips Medical Systems, Best, the Netherlands) with patients in the prone position and a dedicated phased-array breast coil was used. Bilateral unenhanced fat-suppressed (SPAIR) T2-weighted turbo spin-echo sagittal or axial images were obtained with the following parameters: TR/TE=4502/77–4788/120, flip angle=90 degree; field of view (FOV)=200×200–300×300 mm; matrix size=436×430–460×430; slice thickness=1.0 mm. T1-weighted spin-echo images were acquired in the axial planes with the following parameters: TR/TE: 563/9, flip angle: 90 degree, 2 mm thickness, 3.2 mm gap, FOV=350×350 mm. Administered bolus injection of Gadolinium-DTPA (0.1 mmol/kg at a rate of 2 mL/s) was followed by a 20-mL saline flush using an automatic injector (Spectris Solaris; Nihon Medrad, Osaka, Japan). Multiphase dynamic contrast-enhanced T1 high-resolution isotropic volume examination (THRIVE) BLADE imaging in steady-state (BLISS) sequences were performed with 1 pre-enhanced and 5 post-enhanced series in sagittal images with the following parameters: TR/TE=3.49/1.89–3.9/2 flip angle 12 degree; field of view (FOV)=200×200–300×300 mm; matrix size=200×200–300×300 cm; slice thickness=1.0 mm, time of acquisition=90 s. The post-processing process, including early subtraction (ie, first post-contrast images minus pre-contrast images) and maximum intensity projection imaging, was performed on the MRI console to evaluate the extent of breast cancer using second-phase dynamic images.

Precontrast and 5 consecutive post-contrast images were transferred to a commercially available CAD system (CadstreamTM version 4.1.3 Confirma, Inc., Kirkland, WA) and processed. The CAD systems compared the pixel intensity values between the pre-contrast and immediate post-contrast medium series with a 50% increase in enhancement as the minimum threshold. The initial phase determined by the signal change between the pre-contrast and second peak post-contrast series was categorized as either slow (<50% increase), medium (50%–100%), or rapid (>100%) enhancement. Delayed phase enhancement type after the peak post-contrast series was categorized as either persistent, plateau, or washout. A color overlay map was assigned to each pixel for different types of delayed enhancement pattern while comparing the immediate and delayed post-contrast medium series. If a pixel value on the delayed series decreased at a rate of >10% relative to the peak

uptake value, the pixel is color coded as red, indicating a washout pattern. If a pixel value increases by  $>10\%$ , the pixel is color coded as blue, indicating a persistent enhancement pattern. If there is a slope between these 2 values, the pixel is color coded as yellow for plateau enhancement. When  $>2$  patterns of enhancement are mixed up in the same lesion, the most suspicious delayed curve type for malignancy (washout $>$ plateau $>$ persistent) was recorded. The peak enhancement percentage was calculated on the lesion at the second peak post-contrast series. Enhancing lesions detected by CAD can be automatically measured by clicking on the lesion (Fig. 1).

### 2.3. Image evaluation

All lesions detected by mammography, US, and MRI were retrospectively assessed and analyzed using a picture archiving and communication system by 2 radiologists with 15 years and 5 years of experience with breast MRI, respectively. At the time of the retrospective review, the radiologists were unaware of the histopathologic results for invasion and clinical information. Initial imaging analysis was performed independently and discrepant cases were discussed in consensus. Two image sets, that is, conventional MR images alone and MR images with MR CAD data, were evaluated. The first session of conventional MRI without CAD implementation was assessed according to the American College of Radiology Breast Imaging Reporting and Data System (ACR BI-RADS) Breast MRI Lexicon.<sup>[16]</sup> Initially, the lesions were classified by mass versus NME on the second peak post-contrast MR image. Subsequently, morphologic characteristics including lesion size, shape (mass: oval, round, or irregular), margin (mass: smooth, irregular, or spiculate), SI on the T2 WI sequence (higher, lower, or indistinctive) compared with the normal contralateral breast parenchyma and enhancement pattern (mass: homogeneous, heterogeneous, or rim; NME: homogeneous, heterogeneous, clumped, or clustered ring), distribution (NME: focal, linear, segmental, regional, multiple regions, or diffuse) were evaluated. On a second session with MR CAD data, the radiologist selected a specific lesion on an MRI scan and then program automatically generated the following details: initial (fast, medium, or slow) and delay (persistent, plateau, or washout) phase enhancement kinetic descriptor; peak enhancement percentage; lesion size calculated via CAD.

Mammographic and ultrasonographic images taken according to the locations of surgically confirmed enhancing lesions on MRI were also evaluated by ACR BI-RADS lexicon.<sup>[16]</sup>

### 2.4. Histopathologic evaluation

Lumpectomy or total mastectomy was performed by 1 of 2 surgeons who had 16 to 19 and 6 to 9 years of breast surgery experience. Histologic diagnosis was made by a pathologist with 16 to 19 years of experience in breast pathology. Pure DCIS meant no microinvasion and sentinel lymph node metastasis. Nuclear grade (1: low, 2: intermediate, and 3: high), presence of invasion, and largest tumor diameter were determined. The presence of comedonecrosis was also recorded.

### 2.5. Statistical analysis

Clinical, pathologic, and radiologic findings were reviewed. The data were entered into a commercially available computerized spreadsheet (Excel 2016; Microsoft, Redmond, WA). The final

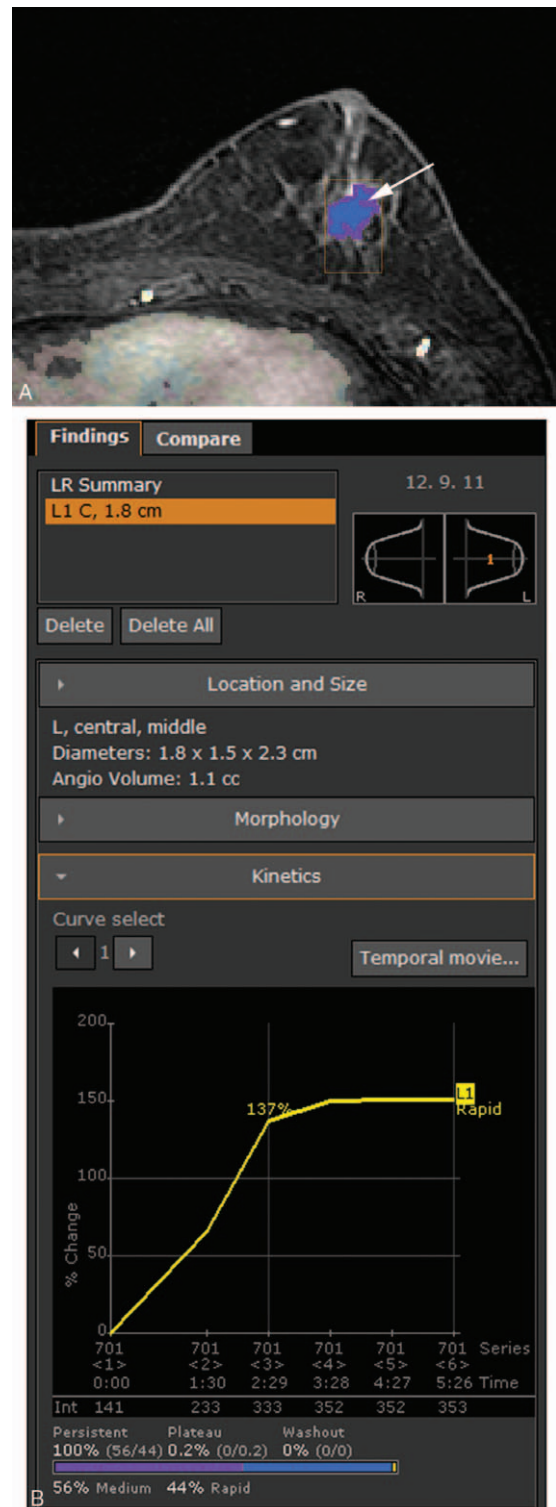


**Figure 1.** A 66-year-old woman with ductal carcinoma in situ in her left breast. (A) Post-contrast T1-weighted imaging with computer-aided diagnosis (CAD) color overlay map showing a slow persistent mass (arrow) detected by CAD. (B) After clicking on the lesion, CAD automatically measured the mass for size, peak enhancement percentile, and early and delayed enhancement kinetics.

radiologic findings and clinicopathologic factors according to the presence of invasiveness in continuous and categorical variables were analyzed using independent *t* test and  $\chi^2$  or Fisher exact test, respectively. A multivariate logistic regression model was used to analyze variables with at least a marginal predictive value ( $P < .05$ ) on univariate analysis. All statistical analyses were performed using commercially available STATA software (version 14.0; StataCorp, College Station, TX) and SPSS (SPSS, version 17.0; SPSS, Chicago, IL). A *P* value of  $< .05$  was considered to indicate a statistically significant difference.

### 3. Results

#### 3.1. Subjects and lesions

Seventy-five (53.2%) of the 141 breasts underwent breast conservation surgery and 66 breasts (46.8%) underwent total mastectomy. Eighty-six (61%) breasts were finally diagnosed as

pure DCIS and 55 (39%) were diagnosed as DCIS-associated invasive cancer. The invasive cancers consisted of 31 micro-invasions, 23 invasive ductal carcinomas, and an invasive papillary carcinoma. The mean histologic diameter of tumor, including DCIS, was  $3.5 \pm 2.3$  cm. In 47 breasts (33.3%), comedonecrosis was present. The nuclear grades of DCIS were 3 for 67 (47.5%), 2 for 61 (43.3%), and 1 for 13 (9.2%) breasts.

#### 3.2. MRI and CAD findings of DCIS groups

Table 1 shows MRI findings for DCIS with or without an invasive component. In the pure DCIS group, lesion size on MRI was smaller than that in the DCIS with an invasive component group ( $2.9 \pm 1.9$  cm vs  $4.1 \pm 2.1$  cm,  $P = .002$ ); the pure DCIS group also showed more homogenous (42.4% [14/33] vs 14.3% [3/21],  $P = .03$ ) internal enhancement characteristics in mass and focal (15.1% [8/53] vs 0% [0/34],  $P = .02$ ) distribution in NME that those shown by the DCIS with an invasive component group.

**Table 1**  
Comparison of MRI and CAD findings between pure DCIS and DCIS combined with an invasive component.

Variables	Total	Pure DCIS (n=86)	Invasive cancer (n=55)	Rate of histologic upgrade (%)	<i>P</i>
MRI findings					
Lesion size on MRI, cm	$3.4 \pm 2.1$	$2.9 \pm 1.9$	$4.1 \pm 2.1$		.002
Mass	54 (38.3)	33 (39.4)	21 (38.2)	38.9	.98
Shape					.74
Round	2 (3.7)	2 (6.1)	0 (0)	0	
Oval	8 (14.8)	5 (15.1)	3 (14.3)	37.5	
Irregular	44 (81.5)	26 (78.8)	18 (85.7)	40.9	
Margin					.78
Smooth	7 (13)	5 (15.2)	2 (9.5)	28.6	
Irregular	34 (63)	21 (63.6)	13 (61.9)	38.2	
Spiculate	13 (24.1)	7 (21.2)	6 (28.6)	46.2	
Internal enhancement Characteristics					.04
Homogenous	17 (31.5)	14 (42.4)	3 (14.3)	17.7	.03*
Heterogeneous	36 (66.7)	19 (57.6)	17 (81)	47.2	.14*
Rim	1 (1.9)	0 (0)	1 (4.8)	100	.39*
Non-mass lesion	87 (61.7)	53 (61.6)	34 (61.8)	39.1	.98
Distribution					.04
Focal	8 (9.2)	8 (15.1)	0 (0)	0	.02*
Linear	3 (3.5)	3 (5.7)	0 (0)	0	.28*
Segmental	64 (73.6)	35 (66)	29 (85.3)	45.3	.051*
Regional	8 (9.2)	5 (9.4)	3 (8.8)	37.5	1*
Multiple regional	1 (1.5)	1 (1.9)	0 (0)	0	1*
Diffuse	3 (3.5)	1 (1.9)	2 (5.8)	66.7	.56*
Internal enhancement Patterns					.1
Homogenous	10 (11.5)	9 (17)	1 (2.9)	10	
Heterogeneous	54 (62.1)	28 (52.8)	26 (76.5)	48.2	
Clumped	14 (16.1)	10 (18.9)	4 (11.8)	28.6	
Clustered ring	9 (10.3)	6 (11.3)	3 (8.8)	33.3	
Signal intensity on T2WI					.06
High	50 (35.5)	26 (30.2)	24 (43.6)	48	
Iso	87 (61.7)	59 (68.6)	28 (50.9)	32.2	
Low	4 (2.8)	1 (1.2)	3 (5.5)	75	
CAD findings					
Early fast enhancement	103 (73.1)	59 (68.6)	44 (80)	42.7	.07
Delay washout	52 (36.9)	17 (19.8)	35 (63.6)	67.3	<.001
Peak enhancement (%)	$219.2 \pm 273.3$	$184.4 \pm 164$	$273.5 \pm 382.5$		.1
CAD detected	129 (91.5)	74 (86.1)	55 (100)	42.6	.004
CAD-detected size, cm <sup>†</sup>	$2.7 \pm 2$	$2.1 \pm 1.6$	$3.4 \pm 2.3$		.001

CAD = computer-aided diagnosis, DCIS = ductal carcinoma in situ, MRI = magnetic resonance imaging, T2WI = T2-weighted imaging.

Note: Data are shown as the number (percentage) of women or as the mean  $\pm$  standard deviation.

\* *P* value from subgroup analysis.

† CAD-detected size was available for 129 CAD-detected lesions.

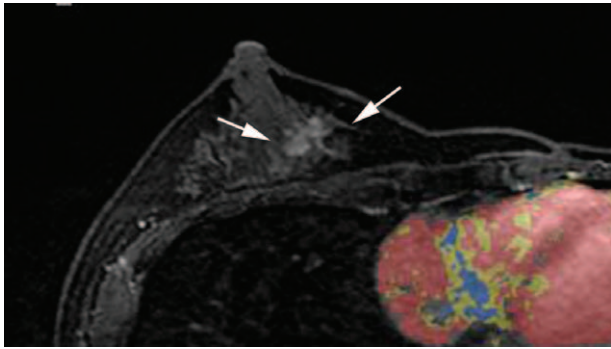


**Figure 2.** A 41-year-old woman with ductal carcinoma in situ (DCIS) in her right breast confirmed via ultrasonography-guided core biopsy. Post-contrast T1-weighted imaging with computer-aided diagnosis (CAD) color overlay map showing a 3-cm regional heterogeneous nonmass lesion (arrows) that was not detected by CAD. Final pathology, as confirmed by lumpectomy, revealed a nuclear grade 1 DCIS measuring 3.4 cm in diameter.

With regard to CAD application, the enhancing mass or NME of the pure DCIS group was less frequently detected (86.1% [74/86] vs 100% [55/55],  $P=.004$ ) (Fig. 2), smaller ( $2.1 \pm 1.6$  cm vs  $3.4 \pm 2.3$  cm,  $p=.001$ ), and showed lesser delay washout kinetics (19.8% [17/86] vs 63.6% [35/55],  $P=.001$ ) (Fig. 3).

### 3.3. Clinicopathologic and other radiologic findings of DCIS groups

Table 2 shows other clinicopathologic factors, mammographic, and ultrasonographic findings according to DCIS with and without an invasive component. The DCIS with an invasive component group was more symptomatic (43.6% [24/55] vs. 23.3% [20/86],  $P=.01$ ); underwent mastectomy more frequently (60% [33/55] vs 38.4% [33/86],  $P=.01$ ); more commonly showed as mass or asymmetry-associated calcifications (27.3% [15/55] vs 11.6% [10/86],  $P=.02$ ) on mammography and mass on US (92.7% [51/55] vs 76.1% [68/86],  $P=.02$ ); and had a larger pathologic tumor size including DCIS ( $4.5 \pm 2.3$  cm vs  $2.9 \pm 2$  cm,  $P < .001$ ), higher prevalence of comedonecrosis (50.9% [28/55] vs 22.1% [19/86],  $P < .001$ ), higher (2 or 3) nuclear grade (2: 29.1% [16/55] vs 52.3% [45/86],  $P=.007$ ; 3: 67.3% [37/55] vs 34.9% [30/86],  $P < .001$ ), and a higher frequency of abnormality detection on mammography (89.1% [49/55] vs 73.3% [63/86],  $P=.02$ ) than the pure DCIS group.

### 3.4. Multivariate analysis

Using multivariate logistic regression analysis, the delay washout kinetics on CAD and pathologic tumor size were independent predictors of the histologic upgrade after adjusting for multiple clinicoradiologic factors (Table 3). The probability of the

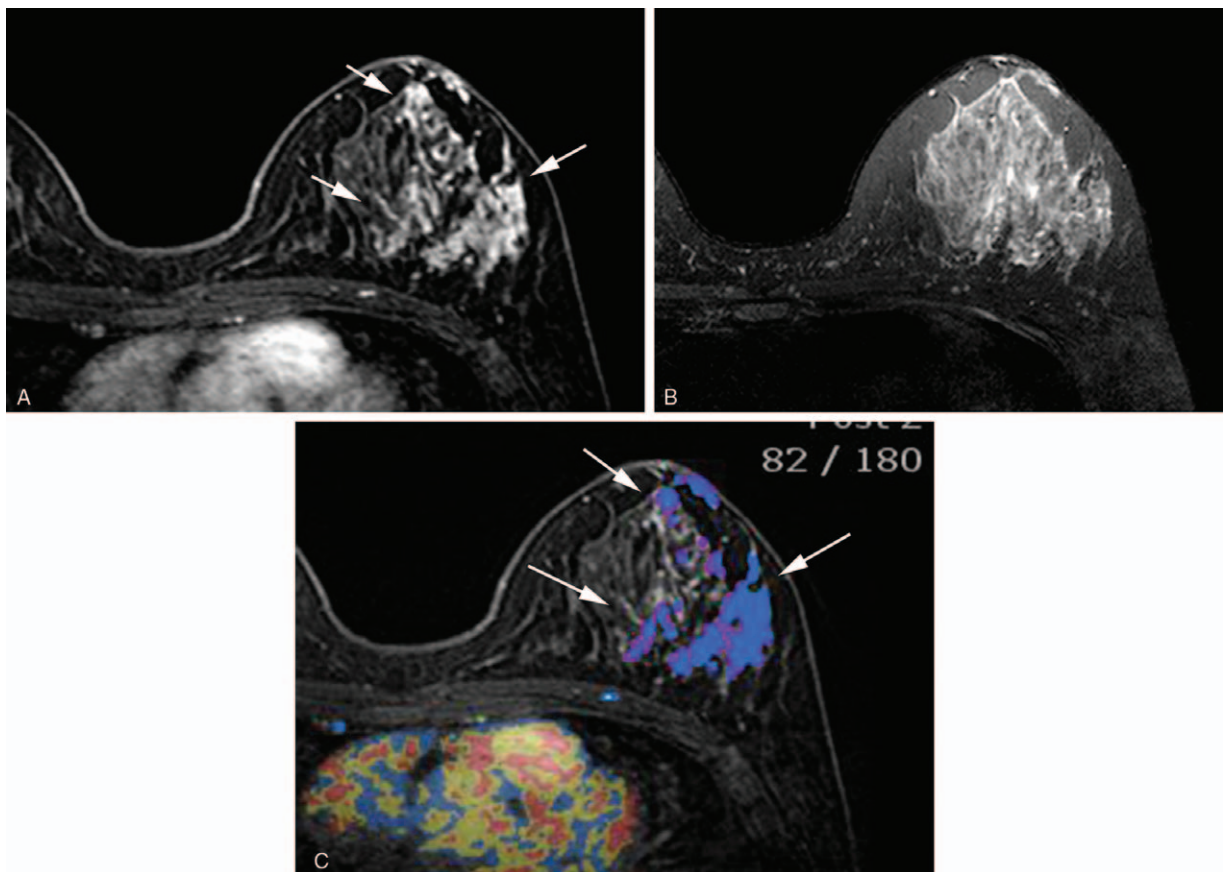


**Figure 3.** A 50-year-old woman with ductal carcinoma in situ (DCIS) in her left breast confirmed via ultrasonography-guided core biopsy. (A) Post-contrast T1-weighted imaging (T1WI) showing a 6.5-cm segmental heterogeneous non-mass lesion (arrows). (B) T2-weighted imaging showing an indistinctive lesion with iso-signal intensity to the adjacent gland. (C) Post-contrast T1WI with computer-aided diagnosis (CAD) color overlay map showing a slow persistent mass (arrows) detected by CAD. The final pathology revealed nuclear grade 3 with comedonecrosis DCIS measuring 6 cm in diameter, as confirmed by mastectomy.

**Table 2**  
**Comparison of variables other than MRI findings between pure DCIS and DCIS combined with an invasive component.**

Variable	Total (n=141)	Pure DCIS (n=86)	Invasive Cancer (n=55)	Rate of histologic upgrade (%)	P
Age, y	51.1 ± 10.6	50.3 ± 10.4	52.2 ± 11.1		.85
Postmenopausal women	60 (42.6)	35 (40.7)	25 (45.5)	41.7	.57
Hormone replacement	15 (10.6)	12 (14)	3 (5.5)	20	.16
Personal history of breast cancer	36 (25.5)	19 (22.1)	17 (30.9)	47.2	.24
Family history of breast cancer	18 (12.8)	13 (15.1)	5 (9.1)	27.8	.43
Dense breast tissue	115 (81.5)	72 (83.7)	43 (78.2)	37.4	.41
Symptomatic	44 (31.2)	20 (23.3)	24 (43.6)	54.6	.01
Total mastectomy	66 (46.8)	33 (38.4)	33 (60)	50	.01
Pathologic size, cm	3.5 ± 2.3	2.9 ± 2	4.5 ± 2.3		<.001
Comedonecrosis	47 (33.3)	19 (22.1)	28 (50.9)	59.6	<.001
Nuclear grade					.001
1	13 (9.2)	11 (12.8)	2 (3.6)	15.4	.07*
2	61 (43.3)	45 (52.3)	16 (29.1)	26.2	.007*
3	67 (47.5)	30 (34.9)	37 (67.3)	55.2	<.001*
Mammographic abnormality	112 (79.4)	63 (73.3)	49 (89.1)	43.8	.02
Mass	14 (9.9)	9 (10.5)	5 (9.1)	35.7	1*
Asymmetry	15 (10.6)	8 (9.3)	7 (12.7)	46.7	.5*
Calcifications	58 (41.1)	36 (41.9)	22 (40)	37.9	.8*
Mass or asymmetry-associated calcifications	25 (17.7)	10 (11.6)	15 (27.3)	27.3	.02*
Ultrasonographic findings					.03
Mass	119 (84.4)	68 (79.1)	51 (92.7)	42.9	
Non-mass lesion	22 (15.6)	18 (20.9)	4 (7.3)	18.2	

DCIS = ductal carcinoma in situ, MRI = magnetic resonance imaging.

Note: The data are shown as the number (percentage) of women or as mean ± standard deviation.

\* P value from subgroup analysis.

presence of invasive components in delay washout kinetics was approximately 4-fold higher (Fig. 4) than that in delay persistent or plateau kinetics (odds ratio [OR], 4.36; 95% confidence interval [CI], 1.96–9.69;  $P = .0003$ ) and increased 1.29-fold according to a 1-cm increase in pathologic size (OR, 1.29; 95% CI 1.05–1.57;  $P = .014$ ) (Fig. 5).

#### 4. Discussion

Here, the CAD application of preoperative MRI findings including detectability on CAD, detected lesion size, and delay washout kinetics were significantly associated with the invasive component in biopsy-proven DCIS. Of the MRI findings, smaller lesion size, homogeneous internal mass enhancement, and focal distribution of NME were significantly associated with pure DCIS. In addition, among the other clinicoradiologic findings, abnormality detection on an ultrasound scan or mammogram, symptomatic condition, patients who underwent total mastectomy, high nuclear grade, and presence of comedonecrosis were significantly correlated with the DCIS-associated invasive component. On multivariate analysis, the probability of the presence of an invasive component was approximately 4-fold higher in delay washout kinetics and had increased 1.29-fold according to 1-cm increase in pathologic tumor size.

**Table 3**  
**Multivariate analysis results of clinicoradiologic factors for predicting the invasive component.**

Variable	Odds ratio	95% Confidence interval	P
Delay washout	4.36	1.96–9.69	.0003
Pathologic size	1.29	1.05–1.57	.014

The final histologic findings from our study revealed 55 invasive lesions of 141 biopsy-proven DCIS and the rate of prevalence of invasive components was 39%. Once DCIS had been diagnosed pathologically during biopsy, knowledge of occult invasion was crucial because it influenced treatment decisions. It has been well known that SLNB should be considered for axillary management in invasive breast cancer patients.<sup>[6]</sup> However, the question of whether to perform SLNB for all biopsy-proven DCIS patients still remained controversial because this would lead to overtreatment.<sup>[7]</sup> Therefore, preoperative prediction of patients at a relatively high risk of invasion was essential to select patients who needed axillary management to avoid a second surgical procedure for axillary nodal staging.

Mammography is a useful screening tool for DCIS but it can only detect calcified portions of DCIS and underestimates the disease extent as opposed to histologic findings.<sup>[17]</sup> The reported diagnostic sensitivity of mammography was only 56%; 48% of occult DCIS escaped detection on mammography.<sup>[18]</sup> In addition, reports about mastectomy specimens revealed that 23% of DCIS cases were multifocal and that preoperative underestimation of disease extent resulted in inadequate excision and positive resection margin.<sup>[19,20]</sup> Many patients with pathologically proven malignant breast lesion underwent noninvasive imaging study, particularly breast MRI, to evaluate the contralateral or multicentric breast lesion. MRI reflects the biology of breast lesions and reveals visual differentiation regarding increased vascularity and capillary permeability of breast lesions. Breast MRI is an emerging complementary work-up tool because of its high sensitivity in the detection of breast lesions and because it provides additional 3-dimensional spatial and temporal information on breast cancer. Recent studies on DCIS have reported the sensitivity values of breast MRI as 97% for 33 patients and 92% for 167 patients.<sup>[18,21]</sup>

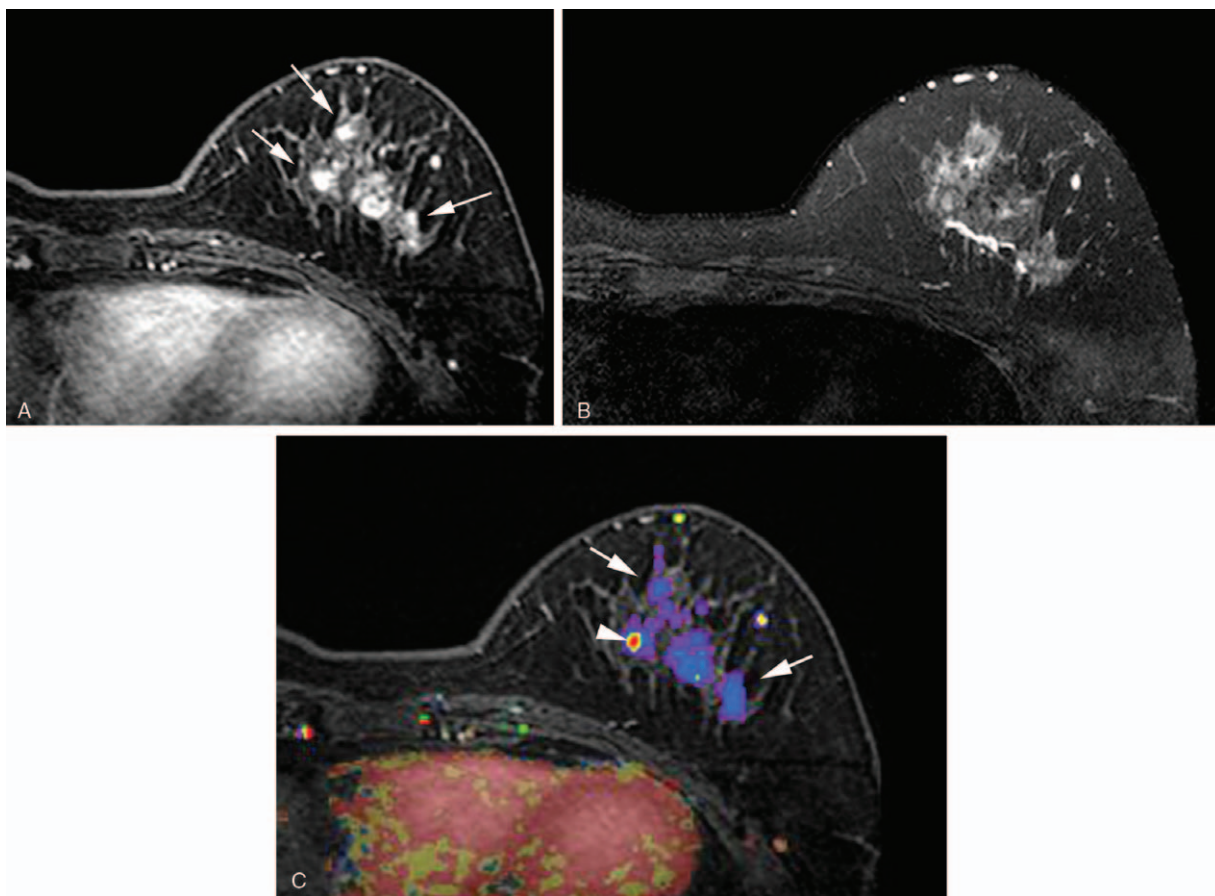


**Figure 4.** A 61-year-old woman with ductal carcinoma in situ (DCIS) in her left breast confirmed via ultrasonography-guided core biopsy. (A) Post-contrast T1-weighted imaging (T1WI) showing a 5.5-cm regional heterogeneous nonmass lesion (arrows). (B) T2-weighted imaging showing that an indistinctive lesion with iso-signal intensity at the adjacent gland. (C) Post-contrast T1WI with computer-aided diagnosis (CAD) color overlay map showing an early enhancing component (arrowhead) with a background of slow persistent enhancement (arrows) detected by CAD. Final pathology revealed a 0.5-cm invasive cancer with 5.5-cm DCIS, as confirmed by mastectomy.

In terms of MRI findings, several previous studies found that lesion size on MRI scans and enhancement pattern of lesions correlated with the co-existence of invasive components in biopsy-proven DCIS. Goto et al and Lamb et al reported that large-size lesions on MRI scans could be associated with an invasive component.<sup>[11,12]</sup> In several studies, authors have analyzed the enhancement pattern and distribution of DCIS on MRI scans and have reported a homogeneous or rim enhancement of lesions, which may help predict the invasive cancer component associated with biopsy-proven DCIS.<sup>[22,23]</sup> In our study, homogeneous enhancement of mass was a significant MRI feature for predicting pure DCIS without invasive cancer and the focal distribution of NME was significantly correlated with pure DCIS rather than with other distributions, including linear or segmental patterns. MRI characteristics such as morphology, enhancement pattern or distribution, and the visual analysis of enhancement kinetics in dynamic contrast-enhanced MRI scans usually facilitated the discrimination between malignant and benign lesions; thus, the MR BI-RADS lexicon may have some limitations for precisely predicting occult invasion in DCIS. Therefore, we applied CAD systems in this study to correctly diagnose invasive cancer. Among the findings, presence of a delayed washout, detectability, or lesion size on CAD were

individually correlated with invasive cancer; the presence of delayed washout was the most predictive MR feature with the highest OR in this study (OR, 4.36; 95% CI, 1.96–9.69;  $P = .0003$ ).

Many previous studies have investigated the predictive factors for an occult invasive component in biopsy-proven DCIS. In a meta-analysis, the authors described how large tumor size, high nuclear grade, presence of symptoms such as palpability, and presence of mammographic abnormalities could be significantly associated with a risk of invasive disease in biopsy-proven DCIS.<sup>[24]</sup> Lee et al reported that large tumor volume and rim or heterogeneous enhancement pattern of the lesion were indicative of the presence of invasive components in biopsy-proven DCIS patients.<sup>[23]</sup> Lamb et al and Marques et al demonstrated that the presence of comedonecrosis in biopsy specimens was a feature associated with invasive components in biopsy-proven DCIS.<sup>[12,25]</sup> In another recent article, the authors suggested that a high nuclear grade was associated with invasive components in patients with a preoperative diagnosis of DCIS.<sup>[13]</sup> Our results were also consistent with the findings of the abovementioned studies, showing that each clinicopathologic feature correlated significantly with the invasive component of biopsy-proven DCIS.

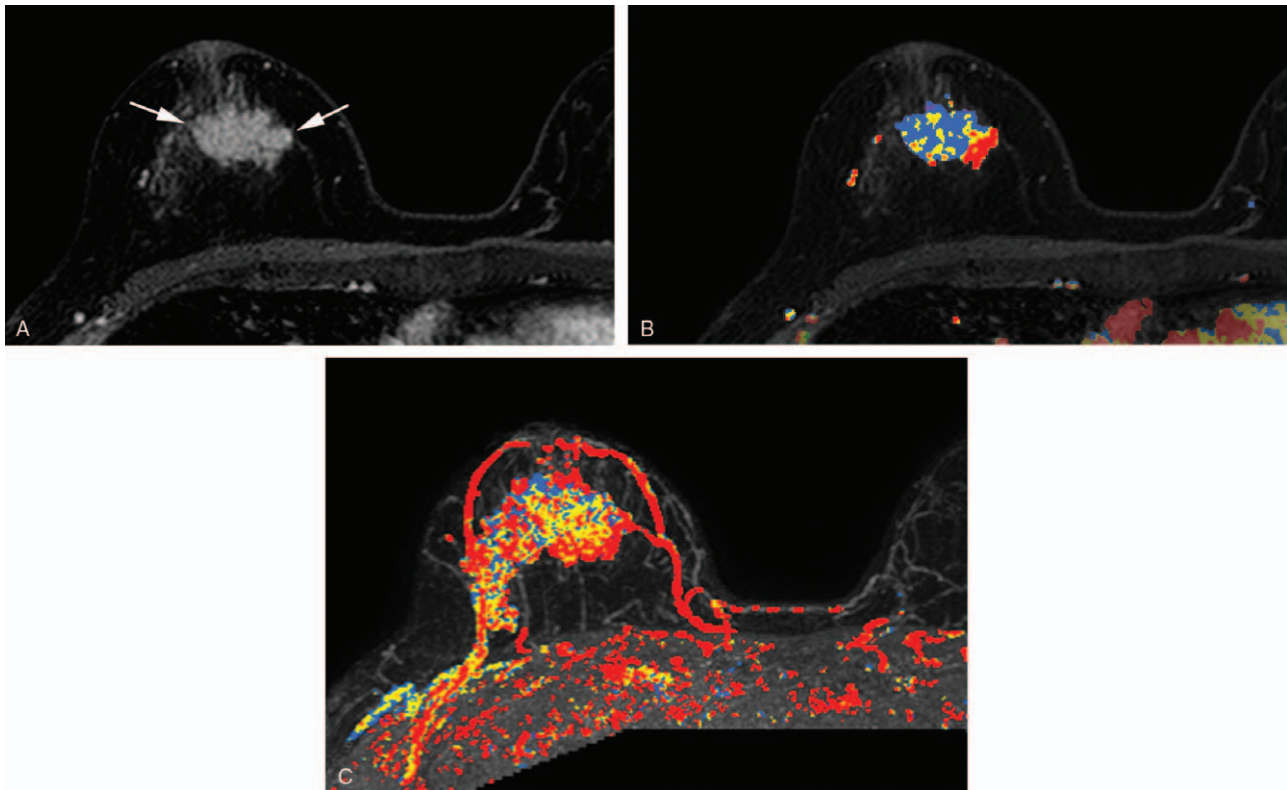


**Figure 5.** A 59-year-old woman with ductal carcinoma in situ (DCIS) in her right breast confirmed via ultrasonography-guided core biopsy. (A) Post-contrast T1-weighted imaging (T1WI) showing a 6.3-cm irregular heterogeneous enhancing mass (arrows). (B, C) Post-contrast T1WI with computer-aided diagnosis color overlay map (B) and maximum intensity projection (C) showing multifocal early fast and delayed washout enhancing components (red colors). Final pathology revealed multifocal invasive ductal cancers with 5.7-cm DCIS, as confirmed by mastectomy.

Our study had several limitations. First, it was performed retrospectively with a small sample size and only included cases of US-guided biopsy-proven DCIS. In addition, we included the patients for about 4 years; therefore, a potential selection bias could have occurred during that period. Second, variable management techniques could have been adopted by different physicians; for instance, there is a potential for variability among the radiologists for deciding whether US-guided core needle biopsy needs to be performed. Third, our study focused on MR features, and thus, we included limited ultrasonographic and mammographic findings in our analysis.

In conclusion, with the application of CAD systems, MRI can be more useful for diagnosing invasive component in patients with biopsy-proven DCIS. As opposed to pure DCIS, DCIS with an invasive component showed a larger pathologic size and a more frequent delayed washout kinetic feature in the CAD system. Therefore, SLNB could be considered for patients selectively.

### Author contributions

**Conceptualization:** Sun Mi Kim.

**Data curation:** Hye Shin Ahn, Bo La Yun, Mijung Jang, Eunyong Kang, Eun-Kyu Kim, Mi Sun Kim.

**Formal analysis:** Eunyong Kang, Eun-Kyu Kim.

**Investigation:** So Yeon Park.

**Methodology:** Sun Mi Kim, Bohyoung Kim.

**Project administration:** Sun Mi Kim.

**Validation:** So Yeon Park.

**Writing – original draft:** Hye Shin Ahn, Mi Sun Kim

**Writing – review & editing:** Bo La Yun, Mijung Jang, Bohyoung Kim.

### References

- [1] Hofvind S, Vacek PM, Skelly J, et al. Comparing screening mammography for early breast cancer detection in Vermont and Norway. *J Natl Cancer Inst* 2008;100:1082–91.
- [2] Virnig BA, Tuttle TM, Shamliyan T, et al. Ductal carcinoma in situ of the breast: a systematic review of incidence, treatment, and outcomes. *J Natl Cancer Inst* 2010;102:170–8.
- [3] Frykberg ER, Bland K. Overview of the biology and management of ductal carcinoma in situ of the breast. *Cancer* 1994;74(1 suppl): 350–61.
- [4] Brennan ME, Turner RM, Ciatto S, et al. Ductal carcinoma in situ at core-needle biopsy: meta-analysis of underestimation and predictors of invasive breast cancer. *Radiology* 2011;260:119–28.
- [5] Kurniawan ED, Rose A, Mou A, et al. Risk factors for invasive breast cancer when core needle biopsy shows ductal carcinoma in situ. *Arch Surg* 2010;145:1098–104.
- [6] Miyake T, Shimazu K, Ohashi H, et al. Indication for sentinel lymph node biopsy for breast cancer when core biopsy shows ductal carcinoma in situ. *Am J Surg* 2011;202:59–65.
- [7] Watanabe Y, Anan K, Saimura M, et al. Upstaging to invasive ductal carcinoma after mastectomy for ductal carcinoma in situ: predictive factors and role of sentinel lymph node biopsy. *Breast Cancer* 2018; 25:663–70.
- [8] Jansen SA, Newstead GM, Abe H, et al. Pure ductal carcinoma in situ: kinetic and morphologic MR characteristics compared with mammographic appearance and nuclear grade. *Radiology* 2007;245:684–91.



- [9] Neubauer H, Li M, Kuehne-Heid R, et al. High grade and non-high grade ductal carcinoma in situ on dynamic MR mammography: characteristic findings for signal increase and morphological pattern of enhancement. *Br J Radiol* 2003;76:3–12.
- [10] Kim JA, Son EJ, Youk JH, et al. MRI findings of pure ductal carcinoma in situ: kinetic characteristics compared according to lesion type and histopathologic factors. *AJR Am J Roentgenol* 2011;196:1450–6.
- [11] Goto M, Yuen S, Akazawa K, et al. The role of breast MR imaging in preoperative determination of invasive disease for ductal carcinoma in situ diagnosed by needle biopsy. *Eur Radiol* 2012;22:1255–64.
- [12] Lamb LR, Lehman CD, Oseni TO, et al. Ductal carcinoma in situ (DCIS) at breast MRI: predictors of upgrade to invasive carcinoma. *Acad Radiol* 2019;doi: 10.1016/j.acra.2019.09.025 [Epub ahead of print].
- [13] Lee KH, Han JW, Kim EY, et al. Predictive factors for the presence of invasive components in patients diagnosed with ductal carcinoma in situ based on preoperative biopsy. *BMC Cancer* 2019;19:1201.
- [14] Cho N, Kim SM, Park JS, et al. Contralateral lesions detected by preoperative MRI in patients with recently diagnosed breast cancer: application of MR CAD in differentiation of benign and malignant lesions. *Eur J Radiol* 2012;81:1520–6.
- [15] Ha T, Jung Y, Kim JY, et al. Comparison of the diagnostic performance of abbreviated MRI and full diagnostic MRI using a computer-aided diagnosis (CAD) system in patients with a personal history of breast cancer: the effect of CAD-generated kinetic features on reader performance. *Clin Radiol* 2019;74:817e815–817. e821.
- [16] Mendelson E, Böhm-Vélez M, Berg W, et al. ACR BI-RADS®. ACR BI-RADS atlas, breast imaging reporting and data system 2013;1–53.
- [17] Rosen EL, Smith-Foley SA, DeMartini WB, et al. BI-RADS MRI enhancement characteristics of ductal carcinoma in situ. *Breast J* 2007;13:545–50.
- [18] Kuhl CK, Schrading S, Bieling HB, et al. MRI for diagnosis of pure ductal carcinoma in situ: a prospective observational study. *Lancet* 2007;370:485–92.
- [19] Harris EE, Schultz DJ, Jones HA, et al. Factors associated with residual disease on re-excision in patients with ductal carcinoma in situ of the breast. *Cancer J* 2003;9:42–8.
- [20] Holland R, Schuurmans Stekhoven JH, Hendriks JH, et al. Extent, distribution, and mammographic/histological correlations of breast ductal carcinoma in situ. *Lancet* 1990;335:519–22.
- [21] Marcotte-Bloch C, Balu-Maestro C, Chamorey E, et al. MRI for the size assessment of pure ductal carcinoma in situ (DCIS): a prospective study of 33 patients. *Eur J Radiol* 2011;77:462–7.
- [22] Park AY, Gweon HM, Son EJ, et al. Ductal carcinoma in situ diagnosed at US-guided 14-gauge core-needle biopsy for breast mass: preoperative predictors of invasive breast cancer. *Eur J Radiol* 2014;83:654–9.
- [23] Lee CW, Wu HK, Lai HW, et al. Preoperative clinicopathologic factors and breast magnetic resonance imaging features can predict ductal carcinoma in situ with invasive components. *Eur J Radiol* 2016;85:780–9.
- [24] Ansari B, Ogston SA, Purdie CA, et al. Meta-analysis of sentinel node biopsy in ductal carcinoma in situ of the breast. *Br J Surg* 2008;95:547–54.
- [25] Marques LC, Marta GN, de Andrade JZ, et al. Is it possible to predict underestimation in ductal carcinoma in situ of the breast? Yes, using a simple score!. *Eur J Surg Oncol* 2019;45:1152–5.